CARDIAC

Association between myocardial hypoxia and fibrosis in hypertrophic cardiomyopathy: analysis by T2* BOLD and T1 mapping MRI

Kiyoe Ando[1] · Michinobu Nagao[2] · Eri Watanabe[1] · Akiko Sakai[1] · Atsushi Suzuki[1] · Risako Nakao[1] · Umiko Ishizaki[2] · Shuji Sakai[2] · Nobuhisa Hagiwara[1]

Abstract

Objectives We assessed whether an association exists between myocardial oxygenation and myocardial fibrosis in patients with hypertrophic cardiomyopathy (HCM), using blood-oxygen-level-dependent (BOLD) T2* cardiac magnetic resonance imaging (T2*-CMR) and T1 mapping.

Methods T1 mapping and T2*-CMR data were collected from 55 HCM patients using a 3-T MR and were prospectively analyzed. T2*-CMR was conducted using the black blood, breath-hold, multi-echo, and gradient echo sequence. Over 10 min, inhalation of oxygen at the flow rate of 10 L/min, T2* for mid-septum was measured following room-air and oxygen inhalation, and ΔT2* ratio (T2*oxy-T2*air/T2*air, %) was calculated. During pre- and post-gadolinium enhancement, native T1 (ms) and extracellular volume fractions (ECV, %) were calculated at sites same as the T2* measurement. Hypoxia was defined as the segment with an absolute value of the ΔT2* ratio $\geq 10\%$.

Results ΔT2* ratio was significantly higher for segments with native T1 ≥ 1290 ms than those with native T1 < 1290 ms ($21 \pm 32\%$ vs. $8 \pm 6\%$, $p = 0.005$). ΔT2* ratio was also significantly higher for segments with ECV $\geq 28\%$ than those with ECV $< 28\%$ ($21 \pm 32\%$ vs. $8 \pm 8\%$, $p = 0.0003$). ROC curve analysis revealed that ΔT2* ratio could detect segments with native T1 ≥ 1290 ms and ECV $\geq 28\%$ and c-statistics of 0.72 and 0.79. According to the multivariate logistic regression analysis results, ECV is an independent factor in hypoxia (odds ratio, 1.47; 95% confidence interval, 1.02–2.13; $p < 0.05$).

Conclusions Analysis of BOLD T2*-CMR and T1 mapping revealed that ECV is strongly associated with ΔT2* ratio, suggesting that the onset of myocardial fibrosis is related to hypoxia in HCM patients.

Trial registration Our study was approved by the ethics committee of our institute (#4036, registered on 21 July 2016)

Key Points

• *Analysis of ΔT2* ratio and ECV with BOLD-T2* and T1 mapping revealed a strong association between myocardial fibrosis and hypoxia in HCM patients.*

Keywords Hypertrophic cardiomyopathy · Functional magnetic resonance imaging · Hypoxia · Fibrosis

Abbreviations

ΔT2*	The difference between T2*oxy and T2*air
ΔT2* ratio	T2*oxy-T2*air/T2*air
BOLD-MRI	Blood-oxygenation-level-dependent magnetic resonance imaging
CMR	Cardiac magnetic resonance imaging
ECG	Electrocardiogram
ECV	Extracellular volume fraction
HCM	Hypertrophic cardiomyopathy
HF	Heart failure
IR	Inversion recovery
LGE	Late gadolinium enhancement
LV	Left ventricle
LVEDV	LV end-diastolic volume
LVEF	LV ejection fraction

✉ Michinobu Nagao
nagao.michinobu@twmu.ac.jp

[1] Department of Cardiology, Tokyo Woman's Medical University, Tokyo, Japan

[2] Department of Diagnostic Imaging & Nuclear Medicine, Tokyo Woman's Medical University, 8-1 Kawada-cho, Shinjuku-ku, Tokyo 162-8666, Japan

LVESV	LV end-systolic volume
MOLLI	Modified Look-Locker inversion recovery
T2*air	T2* Measurement during room-air inhalation
T2*-CMR	T2* Cardiac magnetic resonance imaging
T2*oxy	T2* Measurement after inhalation of supplemental oxygen

Introduction

Hypertrophic cardiomyopathy (HCM) is a relatively common genetic myocardial disease. Many patients have long-term asymptomatic or mild symptoms. However, the estimated mortality was 15% at 5 years and 35% at 10 years, and causes of death include heart failure and fatal arrhythmia [1–3]. One of the causes of fatal arrhythmia is thought to be myocardial fibrosis. O'Hanlon et al reported 136 (63%) of 217 consecutive HCM patients showed fibrosis [4]. Fibrosis is a poor prognostic factor, and it is significant to detect fibrosis in HCM patients [5].

Late gadolinium enhancement (LGE) using cardiac magnetic resonance imaging (CMR) is a non-invasive technique that can identify myocardial fibrosis in patients. Broad LGE area is often seen in high-risk patients with HCM [6]. T1 mapping CMR has also emerged as a quantitative method for evaluating myocardial fibrosis, and the technology has been applied clinically [7–9]. Extracellular volume fraction (ECV) derived from contrast-enhanced T1 mapping is also used to measure the proportion of extracellular space between myocytes and also enables the assessment of diffuse lesions [10].

Tissue hypoxia plays a vital role in the development and progression of various organ diseases. In 1990, Ogawa et al demonstrated blood-oxygenation-level-dependent magnetic resonance imaging (BOLD-MRI) can be used to monitor tissue oxygenation in the brain [11]. Since then, in many BOLD-MRI studies for the heart, stress tests such as use of dipyridamole or breathing maneuvers have been conducted [12–14]. However, these methods may cause asthma attacks and drug allergies. We prioritize reducing patient burden over invasive method such as drugs and breathing maneuvers.

Nagao et al reported oxygen-inhalation T2*-BOLD-MRI has been proposed as a unique quantification method for assessing myocardial oxygenation [15]. Oxygen inhalation is safer and easier than loading drugs or breathing maneuvers used in previous studies. Myocardial oxygenation is defined as the difference in T2* of the myocardium ($\Delta T2* = T2*oxy-T2*air$, ms) between room-air and oxygen inhalation. In refractory heart failure, through using a cardiopulmonary exercise test, it can be seen that $\Delta T2*$ correlates with peak VO_2 or the O_2 pulse [15]. This suggests that $\Delta T2*$ is associated with myocardial hypoxia or oxygen metabolism. Regarding the etiology of fibrosis, collagen 1 expressed by hypoxia drives myocardial fibrosis in HCM. Hypoxia-induced epigenetic modifications are associated with cardiac tissue fibrosis and the development of a myofibroblast-like phenotype [16, 17]. These findings suggest that hypoxia promotes fibrosis in myocardial tissue. This study aimed to investigate potential correlation between fibrosis and hypoxia by using T1 mapping, ECV, and oxygen-inhalation T2*-BOLD-MRI.

Material and method

Patients

Fifty-five patients with HCM who had received regular care at our hospital from February 2018 to June 2019 were prospectively enrolled in this study (Table 1). Patients were diagnosed as having HCM as per the guidelines for the diagnosis and treatment of patients with hypertrophic cardiomyopathy [1]. Other cardiomyopathy presentations that have HCM-like manifestations such as the Anderson-Fabry disease, amyloidosis, and hypertensive heart disease were excluded from this study. We also excluded any patients with renal dysfunction (estimated glomerular filtration rate < 30 mL/min/1.73 m^2); patients with a pacemaker or cardioverter-defibrillator; patients with coronary artery disease, iron overload (after anemia treatment, thalassemia, sickle cell disease, aplastic anemia, and myelodysplasia), and respiratory disease; and any patients that had a valve replacement, or catheter ablation. Informed written consent was obtained from each patient before the study that complied with the Declaration of Helsinki and the guidelines of the local institutional review board.

CMR protocol

All participants underwent an MR using a 3.0-T whole-body imager (Ingenia 3T; Philips Healthcare). This was equipped with dual-source parallel radiofrequency transmission, 32-element cardiac phased-array coils for radiofrequency reception, and cardiac gating with a 4-lead vector electrocardiogram. Firstly, cine balanced turbo field echo sequences in 2-, 3-, and 4-chamber views, as well as a stack of short-axis images, were acquired in parallel to the atrioventricular groove from the base to apex. Cine images were used for the quantification of LV function, i.e., LVEF, LV end-diastolic volume (LVEDV), and LV end-systolic volume (LVESV).

The black blood, breath-hold, and gradient echo were used for myocardial T2* measurement with 14 different echo times (TE = 2.3, 3.4, 4.4, 5.5, 6.6, 7.7, 8.8, 9.9, 10.9, 12.0, 13.1, 14.2, 15.3, and 16.4 ms, GRASE T2* sequence, Philips Healthcare). A mid-ventricular short-axis slice was scanned to measure myocardial T2* during room-air inhalation (T2*air). Other sequence parameters were as follows: flip angle 30°, matrix size 200 × 128, sample bandwidth 2275 Hz/

Table 1 Characteristics of 55 patients with HCM

Clinical characteristics		ΔT2*ratio ≥ 10%	ΔT2*ratio < 10%	p value
Male	35 (63.6%)	18 (32.7%)	17 (30.9%)	1.000
Age (years)	58.0 ± 12.8	55 ± 13.5	59.5 ± 11.2	0.048
Body mass index (kg/m^2)	23.3 ± 3.5	22.9 ± 3.9	23.6 ± 3.1	1.000
Systolic blood pressure (mmHg)	126.0 ± 15.5	121.0 ± 15.3	128.0 ± 15.0	0.0151
Diastolic blood pressure (mmHg)	70.0 ± 11.3	70.0 ± 9.0	73.0 ± 13.0	0.152
Heart rate (beat per minute)	65.0 ± 11.0	65.0 ± 9.3	64.5 ± 12.8	0.566
Historical information				
Non-sustained ventricular tachycardia (+)	11 (20.8%)	6 (10.9%)	5 (9.1%)	1.000
Syncope (+)	2 (3.7%)	1 (1.8%)	1 (1.8%)	1.000
Atrial fibrillation (+)	11 (20.8%)	5 (9.1%)	6 (10.9%)	0.736
Hematology parameter				
Hemoglobin (g/dL)	14.5 ± 1.3	14.2 ± 1.3	14.9 ± 1.4	0.177
Brain natriuretic peptide (pg/dL)	70.1 ± 162.7	116.4 ± 205.6	40.2 ± 75.1	0.072
Medication				
ACE-I/ARB	25 (46.3%)	15 (27.3%)	10 (18.2%)	0.425
Beta-blocker	34 (63.0%)	19 (34.5%)	15 (27.3%)	0.780
Calcium-channel blocker	19 (35.8%)	11 (20.0%)	8 (14.5%)	0.775

pixel, slice thickness 8 mm, field of view 320 mm, oversampling positive, and zoom negative. ECG gating was applied on the R-wave as a double inversion recovery (IR) that was extended to the diastolic phase. Following this [15], the same mid-ventricular short-axis slice was scanned after supplemental oxygen had been delivered through a breathing mask at the flow rate of 10 L/min for 10 min using the previously described protocol (T2*oxy). The acquisition time of each T2* measurement was within a breath-hold. This was < 20 s for 14 different field echo data measurements. Supplemental oxygen was administrated to complete the T2*oxy image acquisition. In order to avoid the susceptibility effect from air in the lung as much as possible, the mid-LV septum of short-axis image was selected. In the septum, we manually draw the largest possible ROI so that it never enters the ventricular cavity. We also generated a T2* map for both room-air and supplemental oxygen using a T2* mapping software (Cardiac quantitative map, Philips Healthcare). The mean signal intensity for these ROIs was measured on the T2*air and T2*oxy images with 14 different echo times. It was assumed that the resulting points formed an exponential decay curve, as the image signal decreased as the echo time increased. The difference between T2*oxy, T2*air (ΔT2*), and ΔT2* ratio (ΔT2*/ T2*air, %) was then calculated.

Native T1 and ECV were measured using the modified Look-Locker inversion recovery (MOLLI) T1 map (Cardiac quantitative map, Philips Healthcare) for the same sites of the mid-septum of LV short-axis as the T2* measurements. We used the same ROI for all measurements (T2*oxy, T2*air, native T1, and ECV) in the mid-septum. This was done before and after gadolinium contrast imaging was conducted. Other scan parameters were as follows: field of view, 360 mm; matrix size, 128 × 256; SENSE factor, 2; repetition time, 2.7 ms; echo time, 1.26 ms; slice thickness, 8 mm; flip angle, 10°; TFE factors, 33; and shot mode, single-shot. Post-contrast imaging was performed approximately 12 to 15 min after 0.1 mmol/kg gadoteric meglumine (Magnescope; Guerbet Japan) had been administered. Hematocrit was determined from a venous blood sample taken following the CMR imaging. As proposed by Flett et al, ECV was calculated based on pre- and post-contrast T1 values and hematocrit [18]. A high signal area of 6SD or more of a normal myocardial signal was determined to be LGE positive. The amount of LGE area was measured with the same software as above. LGE area extending to the apex, the mid, and the base of left ventricle was defined as diffuse type. LGE area limited to one area is defined as a local type. The CMR scan protocol is shown in Fig. 1.

Defined values in CMR measurements

In our facility, native T1 for 20 healthy adults is 1250 ± 20.6 ms. The average native T1 and ECV for 55 HCM patients in this study were 1290 ms and 28%. Previous studies reported that native T1 in HCM using 3 T scanner is higher than control. They defined native T1 > 1239 ms and ECV > 29.5% as abnormally elevated in HCM patients [7, 10]. Roy et al reported mean myocardial ECV is 26.6 ± 3.2% in normal people at 3 T CMR [19]. Based on these results, T1 > 1290 ms and ECV > 28% were used as the cutoffs for fibrotic cardiomyopathy in this study.
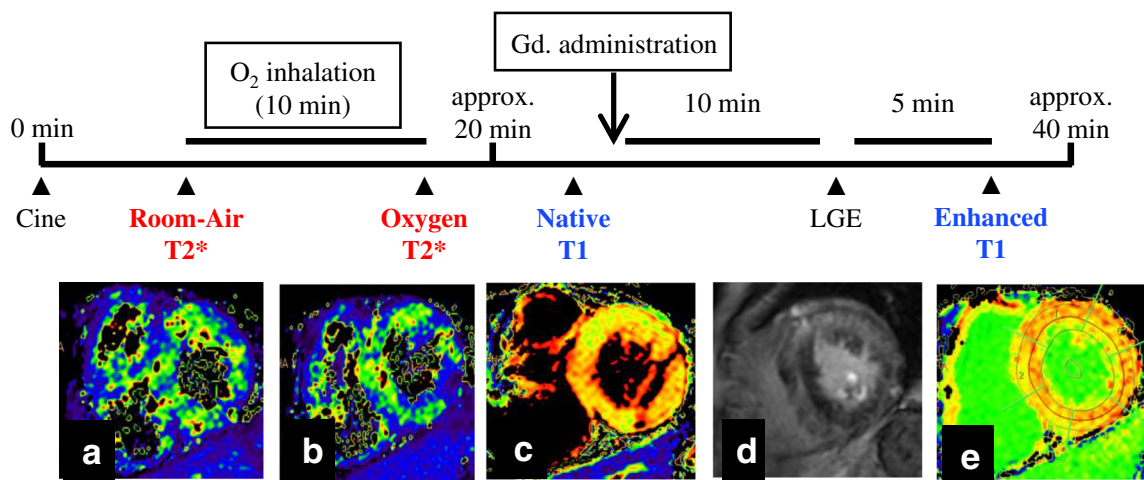
Fig. 1 Cardiac magnetic resonance scan protocol. **a** Room-Air T2*. This image was taken after the cine scan. **b** Oxygen T2*. The image was taken after 10 L of oxygen inhalation for 10 min following T2* imaging. **c** Native T1. Image before gadolinium administration. **d** LGE. Image taken 10 min after gadolinium administration. **e** Enhanced T1. The image was taken 5 min after the LGE scan. T1< 1290ms (N = 28) & ECV< 28% (N = 28)

Based on the results of a previous study taken with the same protocol on a 3 Tesla MRI scanner [15], the baseline T2* was about 30 ms. In injury myocardium of refractory heart failure, the oxygen inhalation changes by the average 3 ms [15]. From these results, 10% or more of ΔT2* ratio was defined as a hypoxic segment.

Reproducibility of CMR measurement

Each parameter was measured by two observers independently (K.A. and M.N). The reproducibility of the CMR-derived measurements for all patients was evaluated by calculating the interobserver variability, defined as the absolute value of the difference between each pair of measurements by the different observers divided by the mean of the measurement pair (expressed as a percentage).

Statistical analysis

Continuous data are expressed as the mean ± the standard deviation. Testing of differences between demographic and clinical data regarding hypoxia (ΔT2* ratio > 10%) and non-hypoxia was accomplished using a variety of tests which were the Mann-Whitney U test for continuous variables and either the Pearson's chi-square test or Fisher's exact test for categorical variables. Comparison of the ΔT2* ratio between the two groups (T1 ≥ 1290 ms or < 1290 ms, ECV ≥ 28% or < 28% and LGE positive or LGE negative) was analyzed using the Mann-Whitney U test. A receiver operating cumulative (ROC) curve analysis was performed to determine the optimal cutoff of the ΔT2* ratio for the detection of a segment with a native T1 ≥ 1290 ms or an ECV ≥ 28%, and to analyze an area under the curve (AUC), a sensitivity, and a specificity. Measures of the association between potentially related variables (age, body mass index, systolic blood pressure, heart rate, hemoglobin, BNP, LVEDV, LVEF, LV mass, septal thick wall, native T1, ECV, LGE, male, ventricular tachycardia, atrial fibrillation, syncope) and the hypoxic segment (ΔT2* ratio > 10%) were first determined using univariate logistic regression. During univariate testing, covariates with $p < 0.05$ were considered for inclusion in a multivariate model that would seek to identify independently associated factors with the hypoxic segment. Covariates were retained during the final multivariate model if the $p < 0.05$ or if they showed evidence of significant confounding or effect modification. Differences between T2*air and T2*oxy for each patient were analyzed using a paired t test. All statistical tests conducted were 2-sided. A p value of < 0.05 was considered to indicate statistical significance. These analyses were performed using the JMP statistical software (version 9.0; JMP, Inc.).

Results

Measurements of T2* and T1 for the ROI in the mid-LV septum of all 55 patients was conducted. A total of 29 patients, or 52.7% (29/55), had hypoxic segments with a ΔT2* ratio > 10%. Twenty-seven patients, or 49% (27/55), had segments with a native T1 ≥ 1290 ms, and 27 patients, or 49% (27/55), also had segments with an ECV ≥ 28%. There were 23 patients (41.8%, 23/55) who had LGE-positive segments in septum.

ΔT2* ratio in segments with and without fibrosis

The ΔT2* ratio was significantly higher for segments with native T1 ≥ 1290 ms than those with native T1 < 1290 ms (21 ± 33% vs. 8 ± 6%, $p = 0.005$). The ΔT2* ratio was also significantly higher for segments with ECV ≥ 28% than those with ECV < 28% (21 ± 32% vs. 8 ± 8%, $p = 0.0003$). The
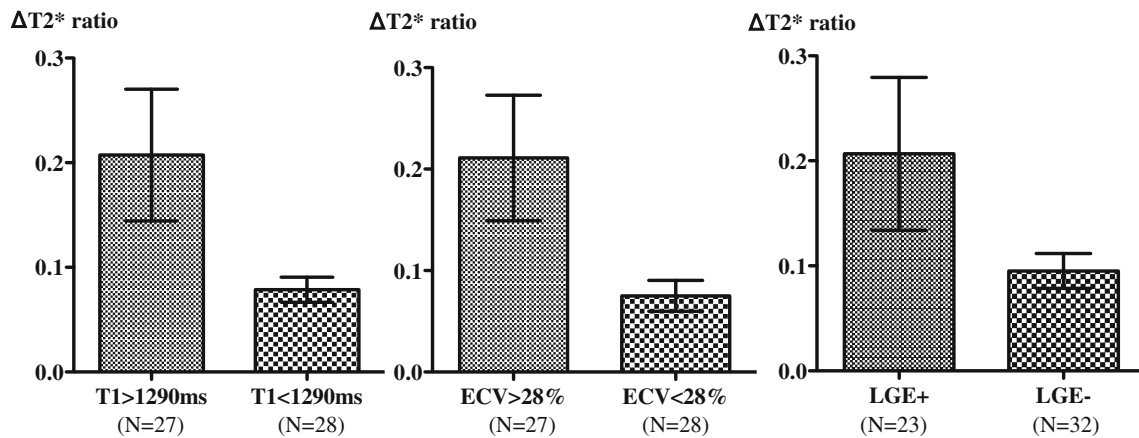
Fig. 2 Comparison of the delta T2* ratio between the positive and negative of each parameter. ΔT2* ratio was significantly higher for segments with native T1 ≥ 1290 ms, ECV ≥ 28%, or LGE positive compared with those with native T1 < 1290 ms, ECV < 28%, or LGE negative (native T1, 21 ± 33% vs. 8 ± 6%, $p = 0.005$; ECV, 21 ± 32% vs. 8 ± 8%, $p = 0.0003$; LGE, 21 ± 35% vs. 10 ± 9%, $p = 0.02$), respectively

ΔT2* ratio was significantly higher for segments with LGE positive compared with those with LGE negative (21 ± 35% vs. 10 ± 9%, $p = 0.02$) (Fig. 2). The ROC analysis showed that using the cutoff of the ΔT2* ratio 10.4% could predict the segments with ECV ≥ 28%, with area under the curves (AUC) of 0.79, 85% sensitivity, and 79% specificity. In addition, the uses of the cutoff of the ΔT2* ratio 14.9% and 8.8% could be predicted that had native T1 ≥ 1290 ms and LGE positive, with AUCs of 0.72 and 0.69, sensitivities of 56% and 83%, and specificities of 89% and 63%, respectively.

Associated factors with hypoxia

Native T1, ECV, and LGE-positive segments were seen to be significantly higher for hypoxic as opposed to non-hypoxic segments. There was no difference observed in the left ventricular functional parameters such as the ejection fraction (Table 2). Potentially related factors for hypoxia were identified using univariate logistic regression (Table 3). Age, the presence of LGE, native T1, and ECV were all identifiable related factors for hypoxia during the univariate logistic regression. However, only ECV (odds ratio, 1.47; 95%

Table 2 MRI measurement of 55 patients with HCM

MRI measurement			ΔT2*ratio ≥ 10%	ΔT2*ratio < 10%	*p* value
Morphology	APH	16 (29.0%)	8 (14.5%)	8 (14.5%)	1.000
	ASH	22 (40%)	9 (16.3%)	13 (23.6%)	0.178
	HOCM	7 (12.7%)	5 (9.0%)	2 (3.6%)	0.426
	dHCM	4 (7.2%)	4 (7.2%)	0	0.113
Left ventricular end-diastolic volume		130.6 ± 38.3	123.7 ± 45.6	133.9 ± 28.9	0.807
Left ventricular end-systolic volume (mL)		51.2 ± 32.4	49.8 ± 41.8	52.1 ± 16.1	0.940
Left ventricular ejection fraction (%)		61.0 ± 10.5	61.0 ± 12.0	61.5 ± 8.4	0.549
Left ventricular mass (g)		105.4 ± 38.1	99.7 ± 44.7	107.3 ± 30.6	0.510
Septal wall thickness (mm)		14.0 ± 5.0	14.0 ± 5.9	14.0 ± 3.9	0.388
Late gadolinium enhancement in mid-septum (+)		23 (41.8%)	18 (32.7%)	5 (9.1%)	0.002
Diffuse LGE		45 (81.8%)	24 (43.6%)	21 (38.1%)	1.000
Focal LGE		10 (18.1%)	5 (9.0%)	5 (9.0%)	
Amount of LGE (%)		12.1 ± 11.4	14.4 ± 14.5	11.8 ± 8.1	0.788
T2*room-air		30.7 ± 4.8	30.2 ± 4.9	30.8 ± 4.7	0.341
T2*oxy		31.6 ± 6.1	32.3 ± 7.3	31.2 ± 4.6	0.757
Native T1(ms)		1290 ± 57.6	1309 ± 63.6	1269.5 ± 37.4	0.0007
Extracellular volume (%)		28.0 ± 4.2	29.0 ± 3.8	26.0 ± 3.4	0.000003

Table 3 Factors associated with hypoxia

Variable	Univariate analysis OR (95% CI)	p value	Multivariate analysis OR (95% CI)	p value
Age (years)	0.96 (0.91–1.00)	0.045	0.96 (0.90–1.01)	0.119
Systolic blood pressure (mmHg)	0.97 (0.93–1.00)	0.085		
Hemoglobin (g/dL)	0.78 (0.52–1.18)	0.238		
Brain natriuretic peptide (pg/dL)	1.01 (1.00–1.01)	0.062		
Left ventricular ejection fraction (%)	0.96 (0.91–1.02)	0.206		
Late gadolinium enhancement (+)	6.87 (2.01–23.5)	0.002	2.85 (0.65–12.6)	0.162
Native TI (ms)	1.02 (1.01–1.04)	0.004	1.01 (0.99–1.03)	0.446
Extracellular volume (%)	1.70 (1.23–2.34)	0.001	1.47 (1.02–2.13)	0.0161

OR, odds ratio; *95% CI*, 95% confidence interval

confidence interval, 1.02–2.13) remained an independent factor of hypoxia during multivariate testing (Table 3).

This study included 16 patients (29%) with apical HCM, 22 patients (40%) with asymmetric septal hypertrophy, 7 patients (12.7%) with hypertrophic obstructive cardiomyopathy, and 4 patients (7.2%) with dilated HCM. There was no difference in the appearance of hypoxia by the subtype (Table 2). This study consisted of 45 patients (82%) with diffuse LGE and 10 patients (18%) with local LGE. There was no difference in the appearance of hypoxia by the two groups (Table 2). In addition, there was no difference in the amount of LGE between hypoxia and non-hypoxia (Table 2).

The change in the T2* from room-air to oxygen inhalation

In all 55 patients, 31 patients had an increased T2*oxy compared with T2*air (56%). In 32 patients without LGE, 22 patients were seen to have increased T2*oxy levels compared with T2*air (69%). There was a significant increase observed in T2* after oxygen inhalation (T2*air vs. T2*oxy, 29.9 ± 4.4 ms vs. 32.4 ± 4.9 ms, $p = 0.0023$). In 23 patients with LGE, 8 patients (34.7%) increased T2*oxy compared with T2*air. Four patients (17.3%) had no change T2*oxy compared with T2*air. Eleven patients (47.8%) decreased T2*oxy compared with T2*air. There was no significant difference seen between T2*air and T2*oxy (31.9 ± 5.2 ms vs. 30.9 ± 7.5 ms, $p = 0.44$) (Fig. 3).

Interobserver variability

Interobserver variability data for the CMR measurements are summarized in Table 4. The mean variability for T2*air, T2*oxy, native T1, and ECV were 4.9%, 5.2%, 0.6%, and 3.3%, respectively.

Fig. 3 The change in T2* from room-air to oxygen inhalation in each LGE scan, both positive and negative. Oxy-T2* significantly increased compared with room-T2* in LGE-negative segments (T2*air vs. T2*oxy, 29.9 ± 4.4 ms vs. 32.4 ± 4.9 ms, $p = 0.0023$). There was no significant difference observed. However, oxy-T2* tended to decrease compared with room-T2* in LGE-positive segments (T2*air vs. T2*oxy, 31.9 ± 5.2 ms vs. 30.9 ± 7.5 ms, $p = 0.44$)
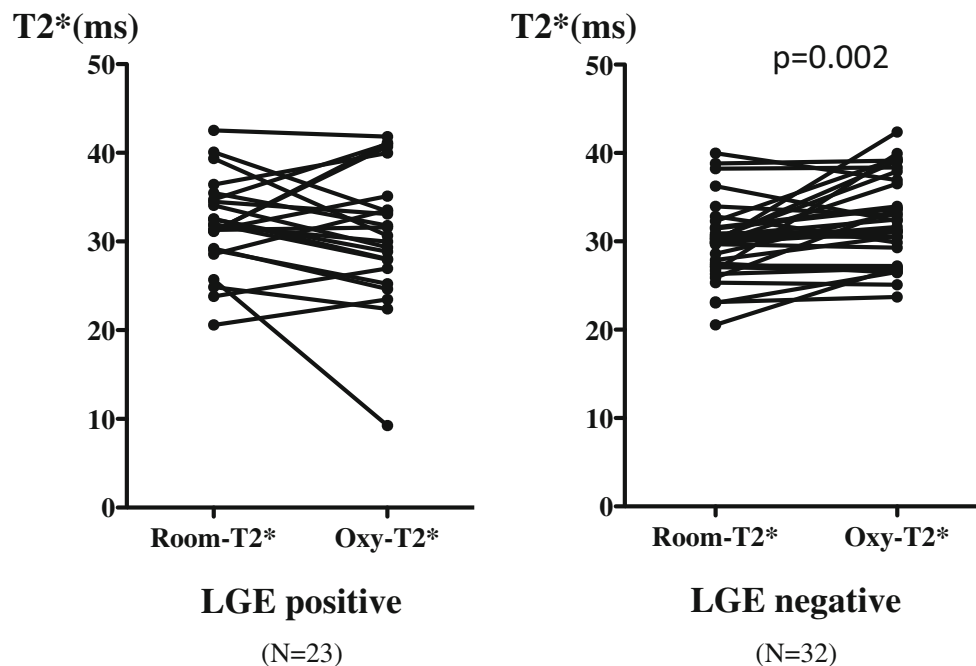
Table 4 Interobserver reproducibility of CMR measurements ($N = 55$)

Parameter	Mean ± SD (%)	Pearson's coefficient (r)
T2*air	4.9 ± 7.4	0.848*
T2*oxy	5.2 ± 9.6	0.839*
Native T1	0.6 ± 1.1	0.908*
ECV	3.3 ± 4.9	0.87*

Data are mean ± standard deviation; *$p < 0.0001$

Discussion

Association with hypoxia and fibrosis

This study shows that myocardial hypoxia derived from T2* BOLD is associated with myocardial fibrosis seen on T1 mapping. ECV was seen to be the most correlated myocardial fibrosis index via CMR associated with hypoxia as expressed as the ΔT2* ratio. Loss of cardiomyocyte due to hypoxia and the myocardial remodeling that compensates are believed to be fibrosis [20]. Impaired myocardial perfusion has been reported as exacerbating fibrosis in patients with HCM [21]. These studies show the association between hypoxia and fibrosis, and our results agree in that point. In the view point of pathogenesis, hypoxic progression is associated with collagen 1 expression in the human cardiac tissue [17]. Ho et al demonstrated that increased collagen 1 is a manifestation of fibrosis in the early stages of HCM. This profibrotic state preceded the development of left ventricular hypertrophy or fibrosis

shown on MRI [16]. This process is thought to be the etiology that hypoxia triggers fibrosis.

In previous MRI studies of the kidney, using a combination analysis of BOLD and diffusion-weighted MRI demonstrated that interstitial fibrosis and hypoxia accelerated the progression of chronic kidney disease [22]. To the best of our knowledge, this is the first study to reveal the relationship between the two factors with BOLD-MRI in human myocardium in vivo.

Effects of oxygen inhalation on blood vessels

Fisher et al reported that hyperventilation alone, and in subsequent combination with prolonged breath-holding has a greater effect on changes in myocardial oxygenation than intravenous administration of adenosine, as assessed by cardiac MRI [14]. They reported when the long breath-hold was performed after hyperventilation, arterial blood CO_2 increases much more rather than a long breath-hold alone. In our study, T2* values were measured during breath-holding for 20–30 s following O_2 inhalation. This protocol is less burdensome than Fisher's method, which involved hyperventilation combined with breath-holding [15]. With CO_2 being the stronger breathing stimulus, prior O_2 inhalation extends the duration of breath-holding by reducing the CO_2 content. Thus, shifting the starting level farther from the threshold at which the breakpoint of breath-holding occurs [23]. Although our protocol has a breath-holding, the participant is not subjected to a high

Fig. 4 Change of oxy-T2* caused by O_2 supply in normal myocardium and injured myocardium. In the normal myocardium (upper row), oxygen inhalation causes vasoconstriction to avoid oxygen overload in the organ along with which blood flow decreases. As a result, the balance between oxy-Hb and deoxy-Hb does not change and does not affect T2*. In hypertrophic myocardium (lower row), even if oxygen is inhaled, the blood vessels have already been expanded due to the chronic ischemic condition, and the blood vessels are poorly reactive, so no vasoconstriction occurs. As a result, the oxygen concentration stagnates as the microcirculation increases. Contrastingly, the oxygen consumption of the organ does not change, so the ratio of oxy-Hb increases and T2*oxy also increases
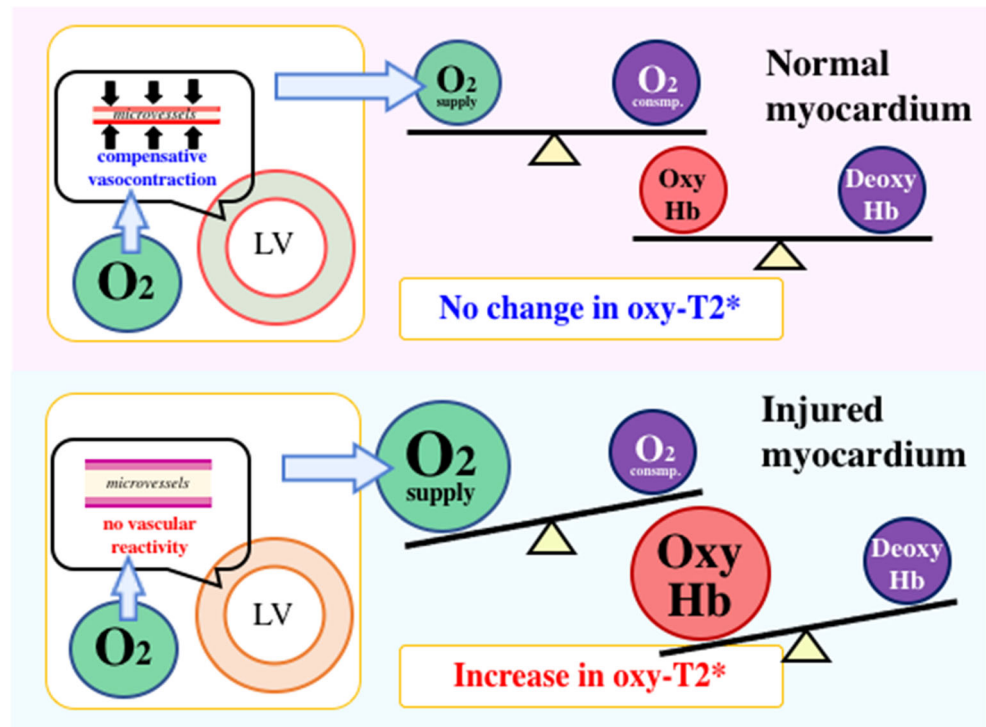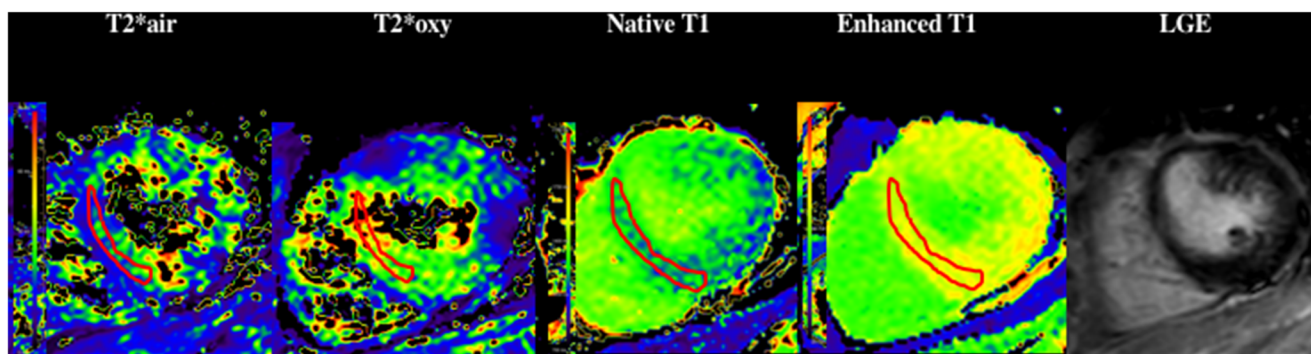
Fig. 5 T2*air map, T2*oxy map, native T1 map, and enhanced T1 map and LGE of mid-LV short-axis images (left to right) for a 51-year-old man showing LGE negative and hypoxia. The red circle in the septum almost corresponds to the ROI. T2* maps show high T2* values as hot color areas and low T2* values as cold color areas. The cold color area in the septum on T2*air changes to the hot color area on T2*oxy. His T2*air and T2*oxy in the ROI are 26.7 ms and 40.0 ms

concentration of CO_2 levels. We think that coronary vasoconstriction effect by CO_2 is small [24].

Mechanism of T2*change after oxygen inhalation

A prior study reported there was no change between T2*air and T2*oxy in healthy adults [15, 25]. In normal myocardium, the inhalation of oxygen causes vasoconstriction in order to avoid oxygen overloading in organ. Furthermore, previous studies have reported a potential adverse physiological effect of supplemental oxygen with reduced coronary blood flow and increased coronary vascular resistance [26, 27]. As a result, the balance between oxy-Hb and deoxy-Hb does not change and therefore does not affect T2* (Fig. 4). In more than half of the patients with HCM (56%), T2* was seen to increase following oxygen inhalation. Additionally, T2*oxy was significantly higher than T2*air in segments without LGE (Fig. 3). In hypertrophic myocardium, even if oxygen is inhaled, the blood vessels have already expanded due to the chronic ischemic condition. Therefore, no vasoconstriction occurs. This results in the oxygen concentration stagnating as the microcirculation flow increases. Contrastingly, the organs' oxygen consumption does not change, so the ratio of oxy-Hb and T2*oxy increases (Figs. 4 and 5). In segments

with LGE, the fluctuation of T2* after oxygen inhalation was high. There was also no constant trend before and after oxygen inhalation (Fig. 3). Oxygen inhalation helps to enable breath-holding longer, which helps with obtaining blur-free T2* images. Pathologically, LGE areas consist of scar fibrosis, micro-hemorrhage, and calcification, which show a low T2* signal. Oxygen inhalation has another effect of showing these lesions with lower T2* signal (Fig. 6).

LVEF and hypoxia in HCM

Most patients in this study preserved systolic function at a low stage of heart failure (NYHA I/II 98%). Only 4 patients in the dilated phase of HCM and had an LVEF < 40% were observed. Their mean ΔT2* ratio was 16.5%. These results reflect hypoxia, even in myocardium with advanced fibrosis and reduced contractility [28].

Limitation

This study has several limitations. First, the cohort came from a single center, and the sample size was small. However, due to the prospective study design, there was no bias in patient selection. Secondly, no control study was conducted in this
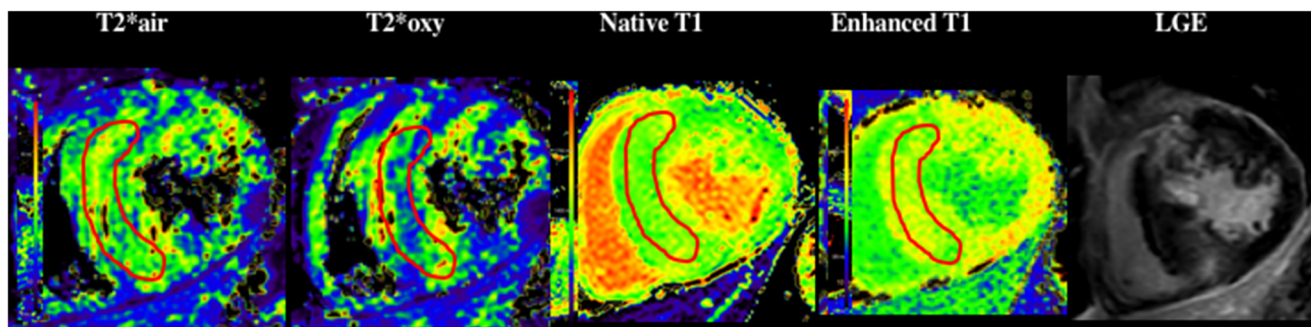

Fig. 6 T2*air map, T2*oxy map, native T1 map, and enhanced T1 map and LGE of mid-LV short-axis images (left to right) for a 46-year-old man showing LGE positive and hypoxia. The yellow area in the septum on T2*air changes to the blue area on T2*oxy. His T2*air and T2*oxy are 39.3 ms and 30.6 ms respectively. LGE areas are seen mainly in right ventricular insertion points of the septum

study. This study was conducted based on past control data that there was no difference between T2*oxy and T2*air in controls (25.5 ± 4.0 ms vs. 25.4 ± 4.4 ms), and that ΔT2* was -0.1 ± 1.3 ms [15]. Thirdly, we did not monitor oxygen saturation during CMR examination. We presume that blood oxygen level is elevated after oxygen inhalation because all patients had no respiratory disease. However, we have not confirmed that. Fourthly, this cross-sectional study could not determine the temporal relationship between hypoxia and fibrosis, and causality cannot be inferred. A future prospective longitudinal study should provide further mechanistic insight [16, 17]. Finally, only the mid-septum in the left ventricle was evaluated. This was done as the mid-septum is less affected by the susceptibility effect, and a stable and reproducible image can be obtained this way. Evaluation of the other segment, especially in the free wall and apex, is presently limited due to magnetic field inhomogeneity.

Conclusion

Simultaneous analysis of T2*-CMR and T1 mapping revealed a temporary association between myocardial fibrosis and hypoxia in patients with HCM. ECV has a strong association with hypoxia as seen using the ΔT2* ratio. The use of T2*-CMR, combined with oxygen inhalation, is a unique technique that assesses myocardial oxygenation. If the constant causality between is proven in subsequent studies, the use of T2*-CMR may be useful for selecting an appropriate treatment option.

Compliance with ethical standards

Guarantor The scientific guarantor of this publication is Prof. Nobuhisa Hagiwara.

Conflict of interest The authors of this manuscript declare no relationships with any companies whose products or services may be related to the subject matter of the article.

Statistics and biometry No complex statistical methods were necessary for this paper.

Informed consent Written informed consent was obtained from all subjects (patients) in this study.

Ethical approval Institutional Review Board approval was obtained.

Methodology
• Prospective
• Cross sectional study
• Performed at one institution

References

1. Geske JB, Ommen SR, Gersh BJ (2018) Hypertrophic cardiomyopathy: clinical update. JACC Heart Fail 6:364–375
2. Hardarson T, De la Calzada CS, Curiel R, Goodwin JF (1973) Prognosis and mortality of hypertrophic obstructive cardiomyopathy. Lancet 2:1462–1467
3. McKenna WJ, Deanfield JE (1984) Hypertrophic cardiomyopathy: an important cause of sudden death. Arch Dis Child 59:971–975
4. O'Hanlon R, Grasso A, Roughton M et al (2010) Prognostic significance of myocardial fibrosis in hypertrophic cardiomyopathy. J Am Coll Cardiol 56:867–874
5. Ommen SR, Gersh BJ (2009) Sudden cardiac death risk in hypertrophic cardiomyopathy. Eur Heart J 30:2558–2559
6. Weng Z, Yao J, Chan RH et al (2016) Prognostic value of LGE-CMR in HCM: a meta-analysis. JACC Cardiovasc Imaging 9: 1392–1402
7. van den Boomen M, Slart R, Hulleman EV et al (2018) Native T1 reference values for nonischemic cardiomyopathies and populations with increased cardiovascular risk: a systematic review and meta-analysis. J Magn Reson Imaging 47:891–912
8. Andrade Gomes HJ, de Padua Vieira Alves V, Nacif MS (2019) The value of T1 mapping techniques in the assessment of myocardial interstitial fibrosis. Magn Reson Imaging Clin N Am 27:563–574
9. Swoboda PP, McDiarmid AK, Erhayiem B et al (2017) Effect of cellular and extracellular pathology assessed by T1 mapping on regional contractile function in hypertrophic cardiomyopathy. J Cardiovasc Magn Reson 19:16. https://doi.org/10.1186/s12968-017-0334-x
10. Ugander M, Oki AJ, Hsu LY et al (2012) Extracellular volume imaging by magnetic resonance imaging provides insights into overt and sub-clinical myocardial pathology. Eur Heart J 33: 1268–1278
11. Ogawa S, Lee TM, Kay AR, Tank DW (1990) Brain magnetic resonance imaging with contrast dependent on blood oxygenation. Proc Natl Acad Sci U S A 87:9868–9872
12. Friedrich MG, Karamitsos TD (2013) Oxygenation-sensitive cardiovascular magnetic resonance. J Cardiovasc Magn Reson 15:43. https://doi.org/10.1186/1532-429X-15-43
13. Wacker CM, Hartlep AW, Pfleger S, Schad LR, Ertl G, Bauer WR (2003) Susceptibility-sensitive magnetic resonance imaging detects human myocardium supplied by a stenotic coronary artery without a contrast agent. J Am Coll Cardiol 41:834–840
14. Fischer K, Guensch DP, Friedrich MG (2015) Response of myocardial oxygenation to breathing manoeuvres and adenosine infusion. Eur Heart J Cardiovasc Imaging 16:395–401
15. Nagao M, Yamasaki Y, Kawanami S et al (2017) Quantification of myocardial oxygenation in heart failure using blood-oxygen-level-dependent T2* magnetic resonance imaging: comparison with cardiopulmonary exercise test. Magn Reson Imaging 39:138–143
16. Ho CY, Lopez B, Coelho-Filho OR et al (2010) Myocardial fibrosis as an early manifestation of hypertrophic cardiomyopathy. N Engl J Med 363:552–563
17. Watson CJ, Collier P, Tea I et al (2014) Hypoxia-induced epigenetic modifications are associated with cardiac tissue fibrosis and the development of a myofibroblast-like phenotype. Hum Mol Genet 23:2176–2188
18. Flett AS, Hayward MP, Ashworth MT et al (2010) Equilibrium contrast cardiovascular magnetic resonance for the measurement of diffuse myocardial fibrosis: preliminary validation in humans. Circulation 122:138–144
19. Roy C, Slimani A, de Meester C et al (2017) Age and sex corrected normal reference values of T1, T2 T2* and ECV in healthy subjects at 3T CMR. J Cardiovasc Magn Reson 19:72. https://doi.org/10.1186/s12968-017-0371-5

20. Segura AM, Frazier OH, Buja LM (2014) Fibrosis and heart failure. Heart Fail Rev 19:173–185

21. Raman B, Ariga R, Spartera M et al (2019) Progression of myocardial fibrosis in hypertrophic cardiomyopathy: mechanisms and clinical implications. Eur Heart J Cardiovasc Imaging 20:157–167

22. Pruijm M, Mendichovszky IA, Liss P et al (2018) Renal blood oxygenation level-dependent magnetic resonance imaging to measure renal tissue oxygenation: a statement paper and systematic review. Nephrol Dial Transplant 33:ii22–ii28

23. Sasse SA, Berry RB, Nguyen TK, Light RW, Mahutte CK (1996) Arterial blood gas changes during breath-holding from functional residual capacity. Chest 110:958–964

24. Guensch DP, Fischer K, Flewitt JA et al (2014) Breathing manoeuvre-dependent changes in myocardial oxygenation in healthy humans. Eur Heart J Cardiovasc Imaging 15:409–414

25. Goldfarb JW, Hsu B, Cao JJ (2019) Effects of supplemental oxygen on cardiovascular magnetic resonance water proton relaxation time constant measurements (T1, T2 and T2*). Magn Reson Imaging 61:124–130

26. Farquhar H, Weatherall M, Wijesinghe M et al (2009) Systematic review of studies of the effect of hyperoxia on coronary blood flow. Am Heart J 158:371–377

27. Kenmure AC, Murdoch WR, Beattie AD, Marshall JC, Cameron AJ (1968) Circulatory and metabolic effects of oxygen in myocardial infarction. Br Med J 4:360–364

28. Travers JG, Kamal FA, Robbins J, Yutzey KE, Blaxall BC (2016) Cardiac fibrosis: the fibroblast awakens. Circ Res 118:1021–1040